International Journal of Dynamics and Control (2021) 9:679–688
https://doi.org/10.1007/s40435-020-00696-x

Walking task space control using time delay estimation based sliding mode of position Controlled NAO biped robot

Yassine Kali[1] · Maarouf Saad[1] · Jean-François Boland[1] · Jonathan Fortin[1] · Vincent Girardeau[1]

Received: 5 May 2020 / Revised: 10 September 2020 / Accepted: 17 September 2020 / Published online: 6 October 2020

Abstract
This work proposes a simple technique to implement in real-time a nonlinear robust controller on a humanoid NAO robot that does not have direct drive joints. The key trick consists of designing a time delay estimation based sliding mode controller without any prior knowledge of the robot's dynamics to alleviate the heavy computations since the on-board processor has low computational power and to deal with the effect of the uncertainties. Then, the calculated torque inputs will be converted to position controller for the servo actuated NAO robot using an appropriate transformer. The proposed method will ensure in addition to high precision tracking a fast convergence during the reaching phase. The proposed control architecture is validated through experimental results on a real NAO robot.

Keywords Sliding mode · Time delay estimation · NAO humanoid robotics · Position controlled servo

1 Introduction

1.1 Context and motivation

Nowadays, the field of humanoid robots has seen revolutionary growth in terms of design, walking control and practical operations. Humanoid robots represent an exciting and interesting topic of research due to their complexity and to their usability in several and hazardous applications where they assist or replace human. Most of the existing humanoid robots use DC servo motors including internal controller as joint actuators. Most of time, the implemented controller consists of the well-known linear Proportional-Integral-Derivative (PID). In this case, only position control based on the kinematics can be achieved. However, this kind of control is not enough to perform a compliant behavior. Moreover, robustness against perturbations is not ensured. For these reasons, a robust dynamic model-based control must be designed.

One of the solutions, to integrate compliance in the humanoid robot walking motion, consists of converting the model-based torque into a model-based position. This solution has been explored and a torque-position transformer based on the identified transfer function of the actuator has been proposed [8,15]. This method has been successfully implemented on the 5-DOF arm of the HONDA ASIMO Humanoid robot. However, the lower body of this humanoid robot was controlled by the Zero Moment Point (ZMP) based stable balance. Therefore, a primary focus of this work is to prove the applicability of this transformer to achieve walking tasks for the lower body of a humanoid robot with position controlled actuators.

As all existing nonlinear systems, the NAO robot [1] is subject to a wide range of matched uncertainties caused by unmodelled dynamics, parameters variation, ground imperfections and disturbances. Therefore, it is mandatory to design a robust nonlinear method that can deal with the effect of uncertainties while ensuring good tracking. Among the most effective and powerful developed controllers in the literature figure the Sliding Mode (SM) control [14]. This latter attracts the researcher due to its interesting features: insensitivity to a large class of non-parametric and parametric uncertainties, simplicity of design and finite-time convergence. The above-mentioned features are a result of using discontinuous switching inputs that drive in a finite-time the trajectories of the commanded system into the designed switching function. Several numerical simulations and practical works have been successfully conducted on several uncertain systems to show the robustness of SM.

✉ Yassine Kali
Yassine.Kali.1@ens.etsmtl.ca

[1] Department of Electrical Engineering, École de Technologie Supérieure, Montreal, QC H3C 1K3, Canada

This approach has been tested through simulations on biped humanoid robot [9,11].

However, two problems remain, the first one is that the system is considered as a linear pendulum [10] which limits the accuracy and the performance while the second one is the major disadvantage of SM that is the chattering phenomenon [2,12]. The latter limits the use of SM in the real world. Indeed, it has been proven that this drawback can introduce many problems as the wear or/and destruction of the moving mechanical components. For the particular case of the NAO robot (v5.0) [4], in the addiction to the fact that this robot does not have direct drive joints, the on-board processor has low computational power and can limit the implementation of any model-based controller due to the huge computation introduced by the dynamics.

1.2 Manuscript organization

The organization of the rest of this manuscript is as follows. Section 2 presents the main contributions of this work. Section 3 describes the model of the considered combined motor-NAO humanoid robot system and discusses the control objective. The design of the proposed nonlinear controller and the model-torque to model-position transformer is explained in Sect. 4. In Sect. 5, experimental studies and their results are described and discussed. Finally, the conclusion is drawn in Sect. 6.

2 Research contribution

As a solution to the aforementioned problems, this work proposes a Time Delay Estimation (TDE) method-based SM control that will be fed to a torque to position transformer. The development of this idea consists of the following three steps:

- In the first step, the whole nonlinear dynamics are reconstructed using TDE method [16]. This method is simple since it uses the delayed available measurements of the system's states and the computed torque inputs. In this paper, the whole dynamics will be estimated to alleviate the heavy computations such as the low computational power of the on-board processor is bypassed.
- In the second step, SM-based Exponential Reaching Law (ERL) and linear term is designed by taking into account the estimated uncertainties to force the system's positions to reach their desired references. The ERL [3] is a famous method that adapts the switching gains of the controller such as the chattering that happens during the sliding phase is reduced. Moreover, the added linear term ensures a faster convergence.

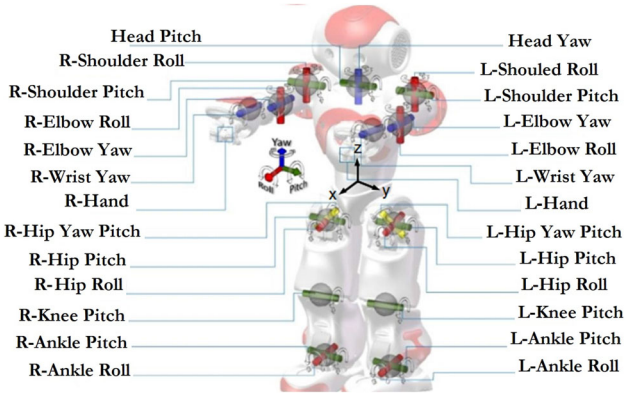

Fig. 1 NAO humanoid robot (v5.0) joints and base frame [1]

- Finally, the third step consists of transforming the computed control law into a position control by using an image (inverse) of the existing linear regulator on the NAO's DC motors since these latter haven't direct drive joints.

3 Preliminaries

The NAO biped robot depicted in Fig. 1 is a humanoid robot that consists of 25 Degrees Of Freedom (DOF) [1]. To walk in all directions, the desired legs joint positions that are fed into the PD position regulator of the DC motors are generated using the classical ZMP, the preview controller on the 3-Dimensional Linear Inverted Pendulum Model (3D-LIPM) [4]. The proposed walking algorithm is stable but does not allow high accuracy, high speed and robustness when the ground is not flat. Therefore, the objective is to develop a nonlinear controller that can handle with these problems. The legs of the NAO robot consists of a combination of 11-DOF, their dynamics is given by [6]:

$$A(q(t))\ddot{q}(t) + B(q(t), \dot{q}(t))\dot{q}(t) + G(q(t)) = \tau(t) \qquad (1)$$

where:

- $\ddot{q}(t),\ \dot{q}(t),\ q(t) \in R^{11}$ are respectively the vectors of joints acceleration, velocity and position;
- $A(q(t)) \in R^{11\times 11}$ is the invertible matrix of inertia;
- $B(q(t), \dot{q}(t)) \in R^{11\times 11}$ is the matrix of centrifugal and Coriolis forces;
- $G(q(t)) \in R^{11}$ is the vector of gravitational forces;
- $\tau(t) \in R^{11}$ is the vector of torque inputs.

All these actuated joints are driven by DC motors. The dynamics of these actuators can be described by:

$$I_M\ddot{q}_M(t) + f_M\dot{q}_M(t) = \tau_M(t) - R\tau(t) \tag{2}$$

where:

- $\ddot{q}_M(t) = \ddot{q}(t)$, $\dot{q}_M(t) = \dot{q}(t) \in R^{11}$ are respectively the vectors of motor or actuated joints acceleration and velocity;
- $I_M = diag(I_{M1}, \cdots, I_{M11})$ is the moment of inertia matrix and $f_M = diag(f_{M1}, \cdots, f_{M11})$ is the viscous matrix;
- $\tau_M(t) \in R^{11}$ is the vector of the motor torque;
- $R = diag(R_1, \cdots, R_{11})$ is the matrix of gear reduction ratio.

Hence, combining (1) and (2) gives:

$$A_0(q(t))\ddot{q}(t) + F(q(t), \dot{q}(t)) = \tau_M(t) \tag{3}$$

where $A_0(q(t)) = RA(q(t)) + I_M$ and $F(q(t), \dot{q}(t)) = RB(q(t), \dot{q}(t))\dot{q}(t) + RG(q(t)) + f_M\dot{q}(t)$.

Introducing a diagonal matrix $\overline{A} \in R^{11\times 11}$ with strictly positive constants that satisfies the following condition:

$$\|I_{11} - A_0^{-1}(q(t))\overline{A}\| < 1 \tag{4}$$

where I_{11} denotes the (11×11) identity matrix. Hence, the combined motor-NAO robot dynamics (3) can be rewritten as:

$$\overline{A}\ddot{q}(t) + H(q(t), \dot{q}(t), \ddot{q}(t)) = \tau_M(t) \tag{5}$$

where:

$$H(q(t), \dot{q}(t), \ddot{q}(t)) = \left[A_0(q(t)) - \overline{A}\right]\ddot{q}(t) + F(q(t), \dot{q}(t)).$$

Let $q_d(t) \in R^{11}$ be the vector of the desired position trajectories and let $\tilde{q}(t) = q(t) - q_d(t) \in R^{11}$ be the vector of the tracking error. The control purpose is to develop a robust stable controller using TDE-based SMC with ERL and then to transform the computed torque into position command by creating an image (inverse) of the existing PD position controller in the NAO biped robot. The design and the stability study of the proposed method will be developed by assuming that the variations of $H_i(q(t), \dot{q}(t), \ddot{q}(t))$ are small during a sufficiently small $\delta\tau$ period of time for $i = 1, \cdots, 11$.

4 Controller design

4.1 Dynamics estimation

In this part, the TDE method will be used to approximate the whole dynamics assumed to be unknown. The basic idea is to alleviate the heavy computations due to the complex robot's dynamics. To this end, the following approximation based on TDE [7,16] is considered:

$$\begin{aligned}\hat{H}(q(t), \dot{q}(t), \ddot{q}(t)) &\cong H(q(t-\delta\tau), \dot{q}(t-\delta\tau), \ddot{q}(t-\delta\tau)) \\ &= \tau_M(t-\delta\tau) - \overline{A}\ddot{q}(t-\delta\tau)\end{aligned} \tag{6}$$

where $\delta\tau$ represents the delay that is mostly chosen to be equal to the sampling time.

Remark 1 The estimation of the vector $H(q(t), \dot{q}(t), \ddot{q}(t))$ requires the measurements of the acceleration of the joint actuators that are often not available. In general, only the position measurements are provided. However, for the NAO biped robot, the user has access to the position and velocity feedback. Therefore, the delayed acceleration can be computed using one of the two following numerical differentiations:

$$\ddot{q}(t-\delta\tau) = \begin{cases} 0, & \text{if } t < \delta\tau \\ \dfrac{1}{\delta\tau}\left[\dot{q}(t-\delta\tau) - \dot{q}(t-2\delta\tau)\right], & \text{if } t \geq \delta\tau \end{cases} \tag{7}$$

4.2 Sliding mode

A detailed study of SM control theory can be found in [13,14]. Succinctly, the first step concerns the design of the sliding surface, the conventional choice for second order systems is as follows:

$$\sigma(t) = \dot{\tilde{q}}(t) + \beta\tilde{q}(t) \tag{8}$$

where β can be selected as a constant or as (11×11) diagonal positive matrix. In the second step, the expression of the control law is derived to guarantee robustness and fast convergence by solving:

$$\dot{\sigma}(t) = -K_1(\sigma(t))\sigma(t) - K_2D(\sigma(t))sign(\sigma(t)) \tag{9}$$

where:

- $K_1(\sigma(t)) = diag\left(K_{1i}\dfrac{\sigma_0}{\sigma_0 + |\sigma_i(t)|}\right)$ with $\sigma_0 > 0$ and $K_{1i} > 0$ for $i = 1, \cdots, 11$;
- $K_2 = diag\,(K_{2i})$ with $K_{2i} > 0$ for $i = 1, \cdots, 11$;
- $D(\sigma(t)) = diag\left(\dfrac{1}{d_i + (1-d_i)\exp^{-|\sigma_i|l_i}}\right)$ with $0 < d_i < 1$ and $l_i > 0$ for $i = 1, \cdots, 11$;
- $sign(\sigma(t)) = [sign(\sigma_1(t)), \cdots, sign(\sigma_{12}(t))]^T$ with $sign(\sigma_i(t))$ is defined by:

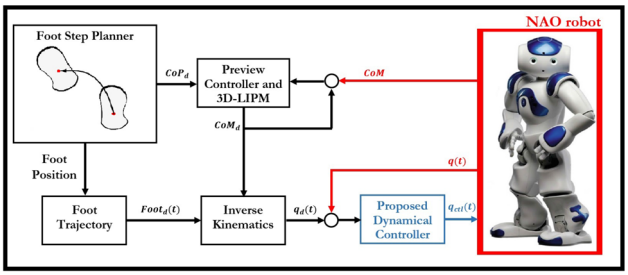

(a) Global architecture.

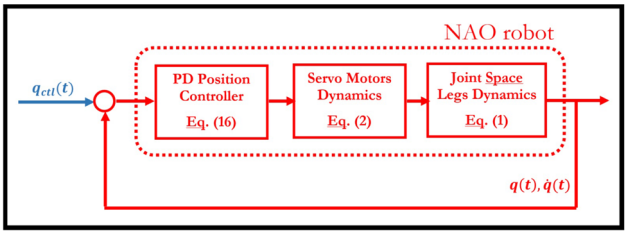

(b) Nao robot.

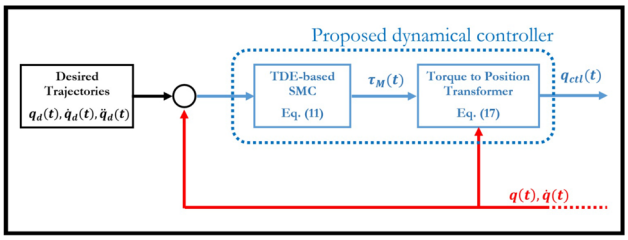

(c) Proposed method.

Fig. 2 Architecture of proposed dynamical control

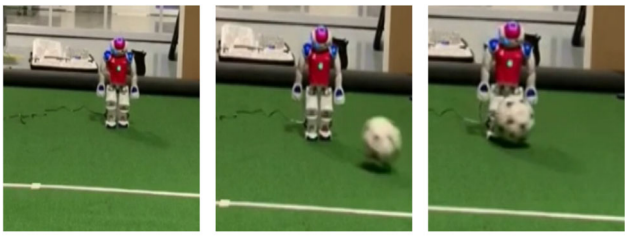

(a) $t \cong 1\ s.$ (b) $t \cong 3\ s.$ (c) $t \cong 4\ s.$

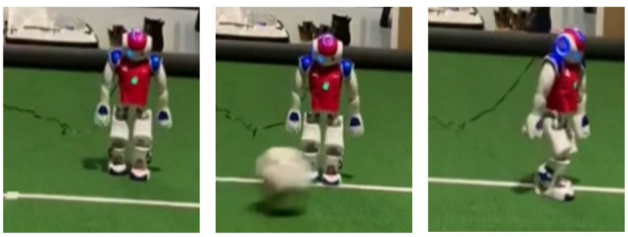

(d) $t \cong 6\ s.$ (e) $t \cong 9\ s.$ (f) $t \cong 12\ s.$

Fig. 3 Sequences of the third scenario

$$sign(\sigma_i(t)) = \begin{cases} -1, & \text{if } \sigma_i(t) < 0 \\ 0, & \text{if } \sigma_i(t) = 0 \\ 1, & \text{if } \sigma_i(t) > 0 \end{cases} \tag{10}$$

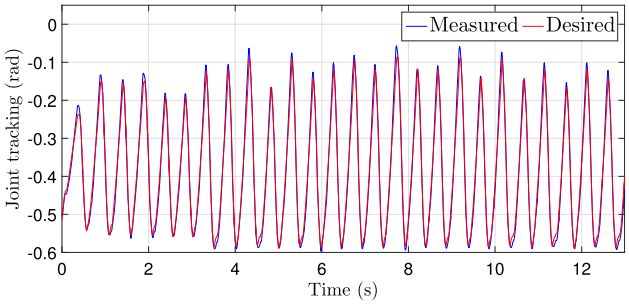

(a) Left hip pitch.

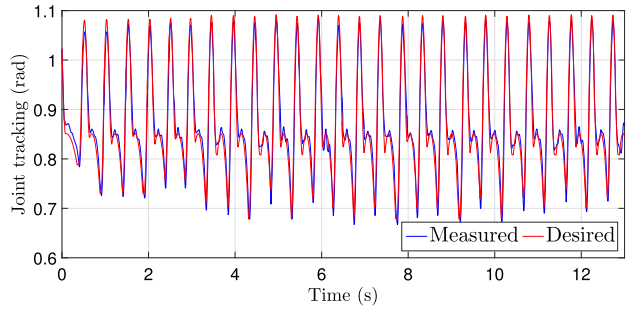

(b) Left knee pitch.

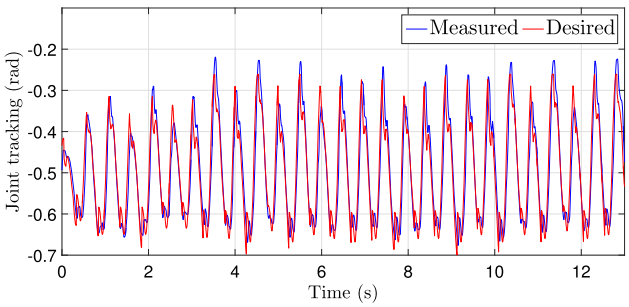

(c) Left ankle pitch.

Fig. 4 Results of joint tracking for the left foot in the first scenario

Theorem 1 *Consider the combined motor-NAO robot dynamics in (5), the control law of the proposed TDE-based SMC obtained by solving (9) as follows:*

$$\begin{aligned} \tau_M(t) = \ & \overline{A}\left[\ddot{q}_d(t) - \beta\dot{\tilde{q}}(t) - K_2 D(\sigma(t))sign(\sigma(t))\right] \\ & -\overline{A}K_1(\sigma(t))\sigma(t) + \hat{H}(q(t), \dot{q}(t), \ddot{q}(t)) \end{aligned} \tag{11}$$

guarantees the convergence of the joint positions to their respective references if the positive gains K_{2i} for $i = 1, \cdots, 11$ are selected as follows:

$$K_{2i} > \frac{|\Delta H_i|}{\overline{A}_{ii}} \tag{12}$$

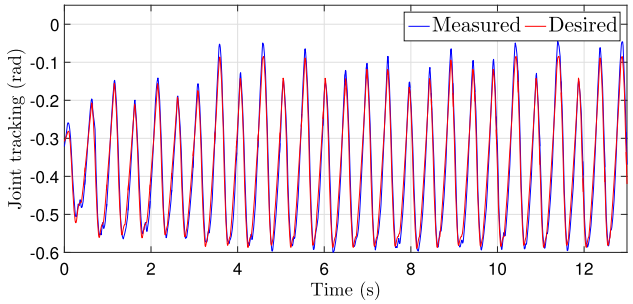

(a) Right hip pitch.

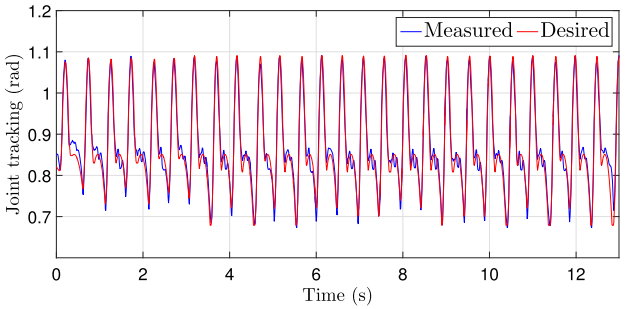

(b) Right knee pitch.

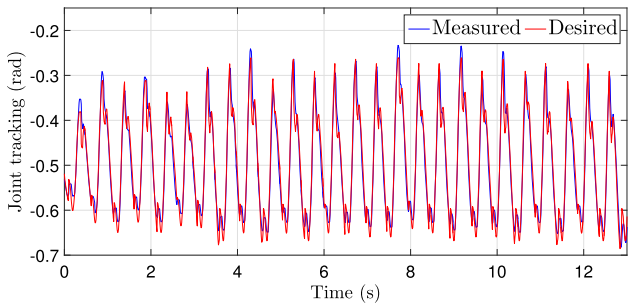

(c) Right ankle pitch.

Fig. 5 Results of joint tracking for the right foot in the first scenario

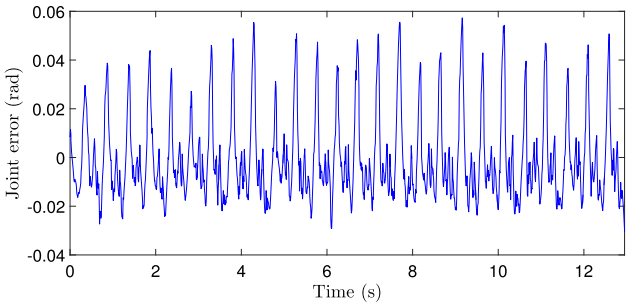

(a) Left hip pitch.

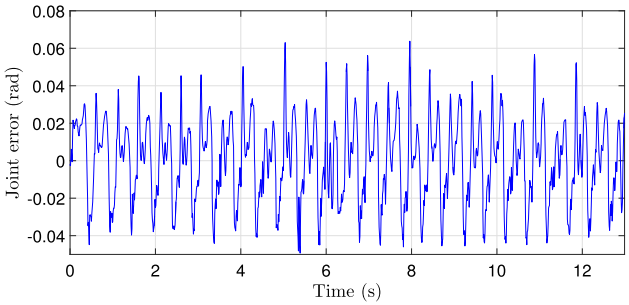

(b) Left knee pitch.

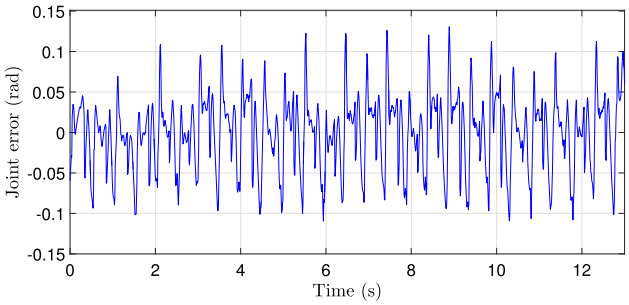

(c) Left ankle pitch.

Fig. 6 Results of joint tracking error for the left foot in the first scenario

where $\Delta H_i = \hat{H}_i(q(t), \dot{q}(t), \ddot{q}(t)) - H_i(q(t), \dot{q}(t), \ddot{q}(t))$ *is the estimation error.*

Proof To analyze the closed-loop system stability, a positive-definite Lyapunov function is selected as follows:

$$V(t) = 0.5\, \sigma^T(t)\sigma(t). \tag{13}$$

Hence, taking the time derivative of (13) yields to:

$$\begin{aligned} \dot{V}(t) &= \sigma^T(t)\dot{\sigma}(t) \\ &= \sigma^T(t)\left[\ddot{q}(t) - \ddot{q}_d(t) + \beta\dot{\tilde{q}}(t)\right] \\ &= \sigma^T(t)\left[\overline{A}^{-1}[\tau_M(t) - H(q(t), \dot{q}(t), \ddot{q}(t))]\right] \\ &\quad + \sigma^T(t)\left[-\ddot{q}_d(t) + \beta\dot{\tilde{q}}(t)\right]. \end{aligned} \tag{14}$$

Substituting the obtained control law (11) in the above equation gives:

$$\begin{aligned} \dot{V}(t) &= \sigma^T(t)\left[\overline{A}^{-1}\Delta H - K_1(\sigma(t))\sigma(t)\right] \\ &\quad -\sigma^T(t)K_2 D(\sigma(t))sign(\sigma(t)) \\ &= \sum_{i=1}^{11} \frac{1}{\overline{A}_{ii}}\sigma_i(t)\Delta H_i - K_{1i}\frac{\sigma_0\sigma_i^2(t)}{\sigma_0 + |\sigma_i(t)|} \\ &\quad - \sum_{i=1}^{11} K_{2i}\frac{|\sigma_i(t)|}{d_i + (1-d_i)\exp^{-|\sigma_i|^{l_i}}} \end{aligned}$$

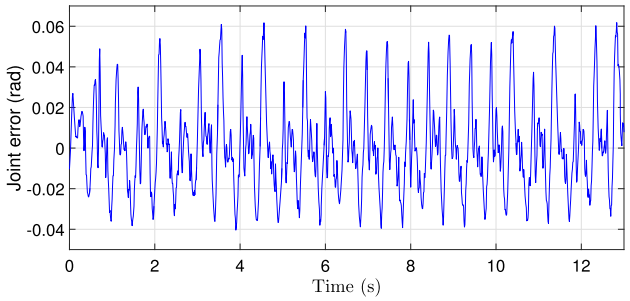

(a) Right hip pitch.

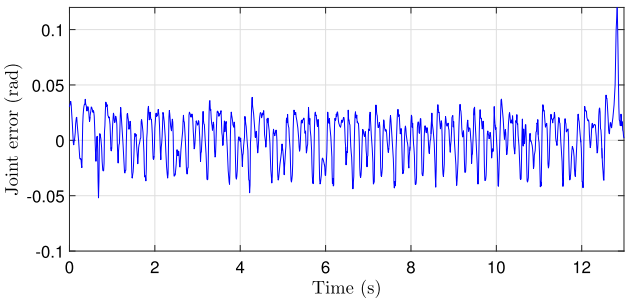

(b) Right knee pitch.

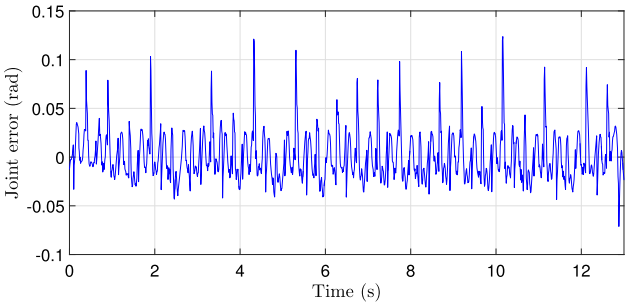

(c) Right ankle pitch.

Fig. 7 Results of joint tracking error for the right foot in the first scenario

$$\leq \sum_{i=1}^{11} \frac{1}{A_{ii}} |\sigma_i(t)||\Delta H_i| - K_{1i} \frac{\sigma_0 \sigma_i^2(t)}{\sigma_0 + |\sigma_i(t)|} - \sum_{i=1}^{11} K_{2i} \frac{|\sigma_i(t)|}{d_i + (1 - d_i) \exp^{-|\sigma_i|^{l_i}}} \tag{15}$$

where $\Delta H = \hat{H}(q(t), \dot{q}(t), \ddot{q}(t)) - H(q(t), \dot{q}(t), \ddot{q}(t))$ is the TDE error. Hence, if the condition in (12) is satisfied, $\dot{V}(t)$ is negative definite. Thus, the stability of closed-loop system is ensured. This completes the proof. □

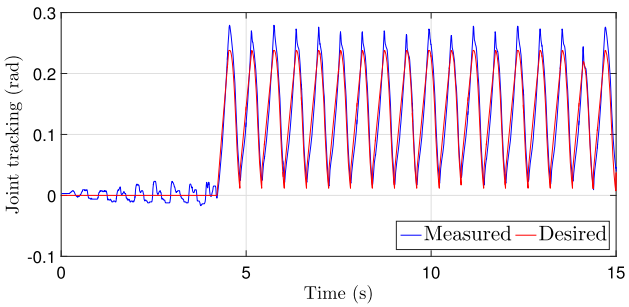

(a) Left hip roll.

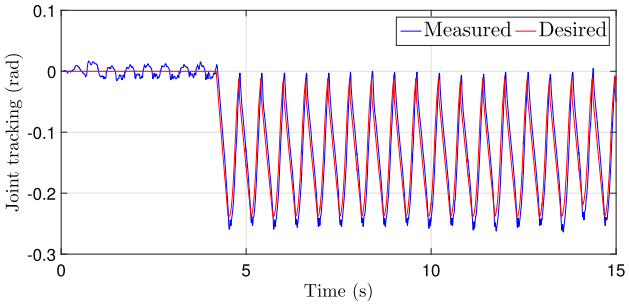

(b) Left ankle roll.

Fig. 8 Results of joint tracking for the left foot in the second scenario

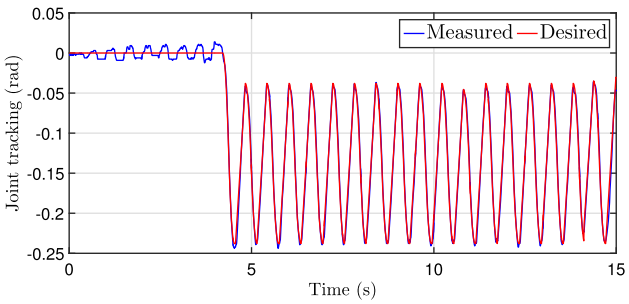

(a) Right hip roll.

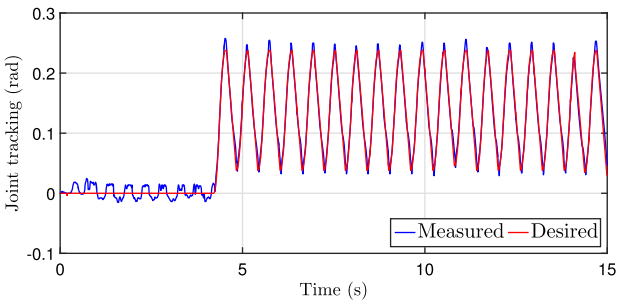

(b) Right ankle roll.

Fig. 9 Results of joint tracking for the right foot in the second scenario

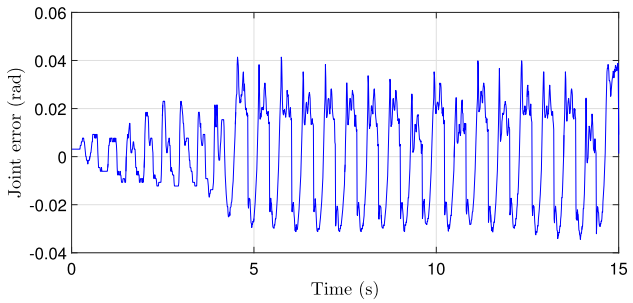

(a) Left hip roll.

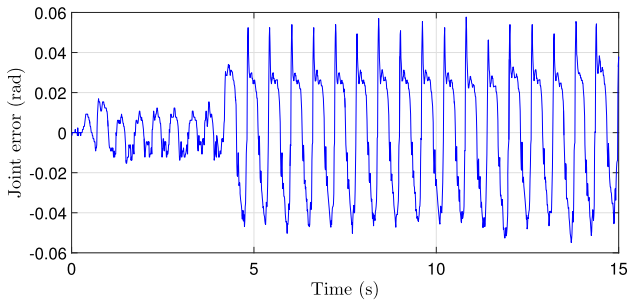

(b) Left ankle roll.

Fig. 10 Results of joint tracking error for the left foot in the second scenario

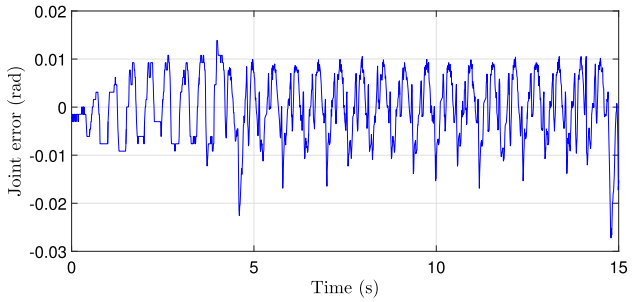

(a) Right hip roll.

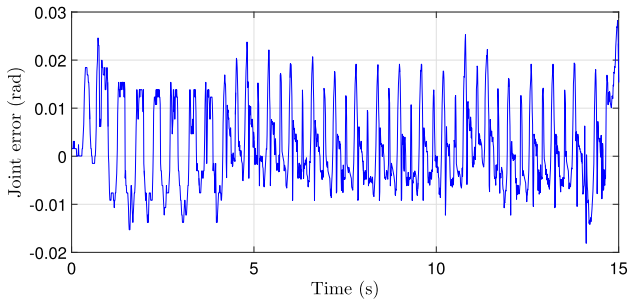

(b) Right ankle roll.

Fig. 11 Results of joint tracking error for the right foot in the second scenario

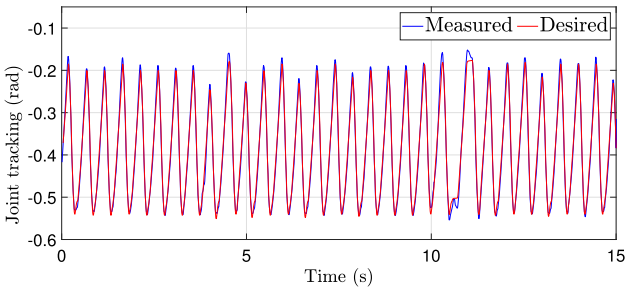

(a) Left hip pitch.

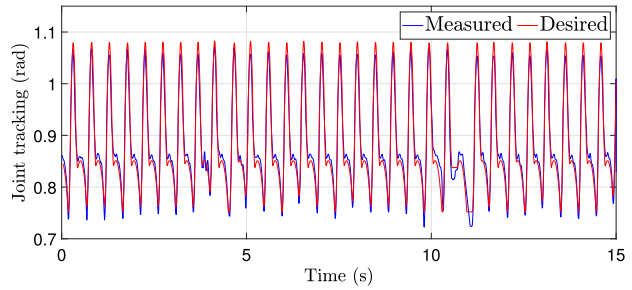

(b) Left knee pitch.

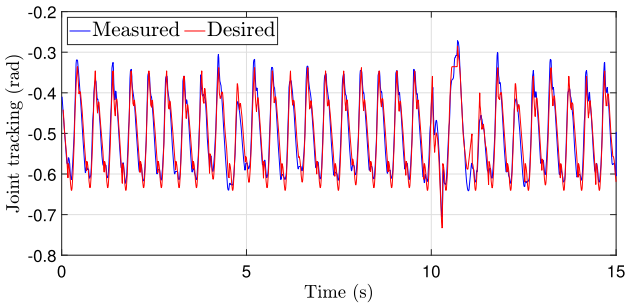

(c) Left ankle pitch.

Fig. 12 Results of joint tracking for the left foot in the third scenario

4.3 Torque to position transformer

The low level regulator in each NAO's DC servo motor is a Proportional-Derivative (PD) such as its output generates the following torque input vector:

$$\tau_M(t) = K_p(q(t) - q_{ctl}(t)) + K_d(\dot{q}(t) - \dot{q}_d(t)) \tag{16}$$

where K_p and K_d are (11×11) diagonal positive matrices that represent respectively the proportional and the derivative gains. Hence, the transformer is obtained by computing the inverse of (16) as follows:

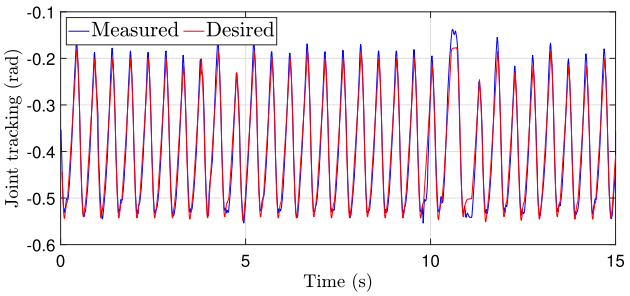

(a) Right hip pitch.

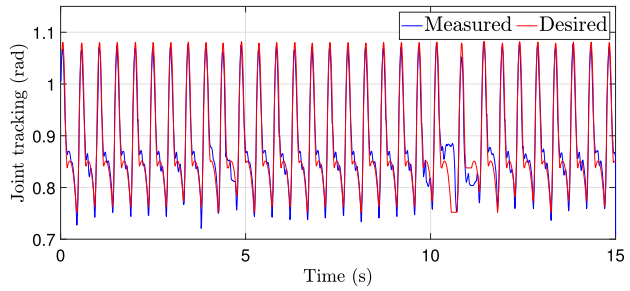

(b) Right knee pitch.

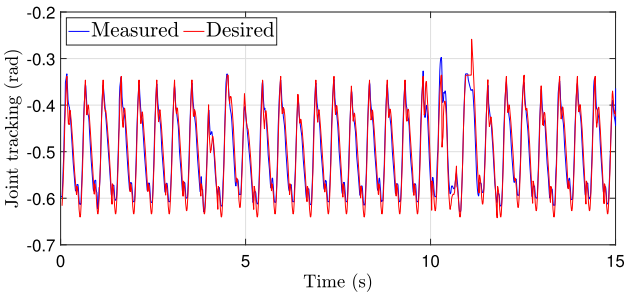

(c) Right ankle pitch.

Fig. 13 Results of joint tracking for the right foot in the third scenario

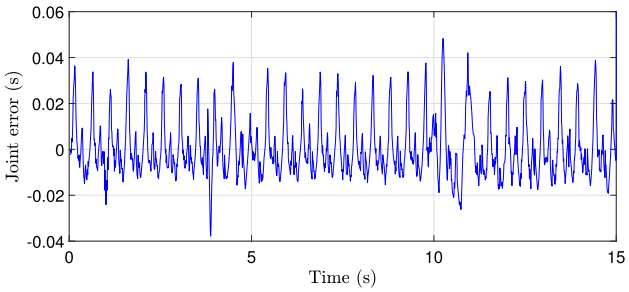

(a) Left hip pitch.

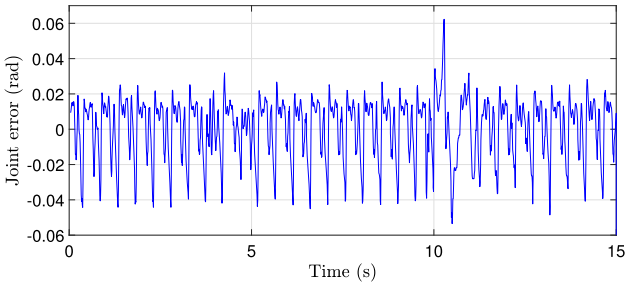

(b) Left knee pitch.

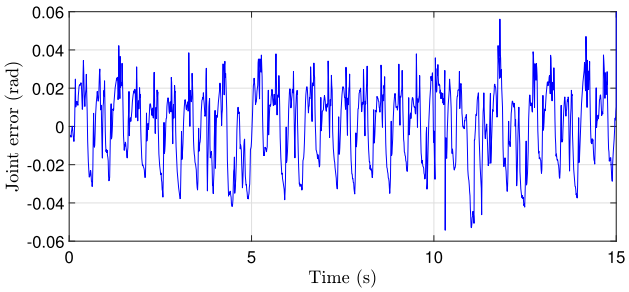

(c) Left ankle pitch.

Fig. 14 Results of joint tracking error for the left foot in the third scenario

$$q_{ctl}(t) = q(t) + K_p^{-1}\left(K_d(\dot{q}(t) - \dot{q}_d(t)) - \tau_M(t)\right). \quad (17)$$

The architecture of the closed-loop system is depicted in Fig. 2 and the steps of its implementation are described in the algorithm below.

Data: Define: β, $\bar{A}$, K_1, K_2, K_p, K_d, σ_0, d_i, l_i, $\tau_M(0)$, Δt, N % number of samples
initialization j==0;
while *j!=N* **do**
  define: $q_d(j)$, $\dot{q}_d(j)$, $\ddot{q}_d(j)$;
  read $q(j)$, $\dot{q}(j)$;
  compute acceleration:
  $\ddot{q}(j) = (\dot{q}(j) - \dot{q}(j-1))/(t(j) - t(j-1))$;
  compute error of position: $\tilde{q}(j) = q(j) - q_d(j)$;
  compute error of velocity: $\dot{\tilde{q}}(j) = \dot{q}(j) - \dot{q}_d(j)$;
  define sliding surface: $\sigma(j) = \dot{\tilde{q}}(j) + \beta\tilde{q}(j)$;
  compute torque $\tau_M(j)$ in (11);
  TDE: $H(j+1) = \tau_M(j) - \bar{A}\ddot{q}(j)$;
  torque to position transformer:
  $q_{ctl}(j) = q(j) + K_p^{-1}\left(K_d\dot{q}(j) - \tau_M(j)\right)$;
  j++;
end

Algorithm 1: Calculate the position controlled $q_{ctl}(t)$

5 Experimental results

This section explains briefly the experimental setup that features the real-time implementation of the proposed position controller applied to the NAO v5.0 humanoid robot. This little 58 *cm* robot is the world's best-selling humanoid. As said

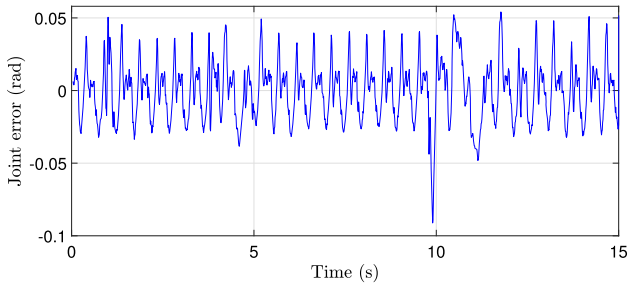

(a) Right hip pitch.

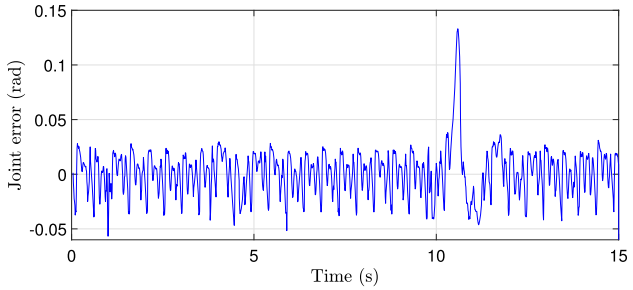

(b) Right knee pitch.

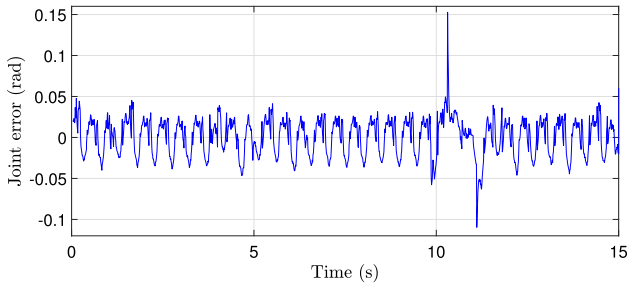

(c) Right ankle pitch.

Fig. 15 Results of joint tracking error for the right foot in the third scenario

before and shown in Fig. 1, the NAO has 25 rotary DOFs reported as follows: 5 DOFs in each leg, 1 common DOF shared by the two legs, 5 DOFs in each arm, 1 DOF in each hand and finally 2 DOFs in the neck. The described DOFs are actuated by DC motors and equipped by position sensors to provide accurate measurements.

The control objective in these three tests is to follow two different trajectories by controlling the 11 DOFs of the legs. In the first scenario, the robot walks straight while he walks on the right side in the second scenario. In the third scenario where the sequences are shown in Fig. 3, the NAO robot walks straight and kicked two times respectively at $t = 4\ s$ and $t = 10\ s$ by an official soccer ball that weighs 450 g. In the above-mentioned cases, a non perfectly flat carpet has been used to create small obstacles. As depicted in Fig. 2, the desired trajectories for a reliable walk task are generated using the existing developed walking engine by Aldebaran Robotics [5]. The proposed controller (11) is performed using C++ programming language.

As all the controller gains are positive constant elements, thus, their setting and tuning are simple. First of all, the diagonal elements of the matrix β of the switching function in (8) is selected to be $\beta_i = 7$ for $i = 1, \cdots, 11$. Then, $\overline{A}_{ii}$ for $i = 1, \cdots, 11$ has been selected sufficiently small and increased gradually until fixed at 0.001, while checking the control performance by trial and error. Then, $K_{2i} = 3$, $d_i = 0.01$ and $l_i = 1$ have been selected through a manual tuning to verify the stability condition and to achieve optimal performance. This choice let the switching gain vary between 3 and 300. Finally, to improve the reaching time the gains of the linear term have been selected as: $K_{1i} = 20$ and $\sigma_0 = 0.0001$.

The experimental results are illustrated in Figs. 4, 5, 6 and 7 for the first scenario, in Figs. 8, 9, 10 and 11 for the second scenario and in Figs. 12, 13, 14 and 15 for the third scenario. The proposed TDE-based SM of position commanded robot ensures a fast convergence of the joint positions to their respective desired references with good accuracy. These results are, thank to the good estimation, since all the dynamics are supposed to be unknown. It can be seen in Figs. 6, 7, 10, 11, 14 and 15 that the tracking error is small. This confirms that the results are satisfactory.

6 Conclusion

In this paper, a robust nonlinear controller based dynamics on a humanoid NAO biped robot has been proposed. The basic idea consists of approximating the whole dynamics and the perturbations using time delay estimation method, then, the sliding mode controller is derived. The proposed scheme is simple and allows the alleviation of the heavy computations due to the complexity of the dynamics. Finally, the computed torque will be transformed into a position controller for the servo actuated NAO robot using an image of the existing PD regulator. The developed controller is validated through experimentation on the real NAO robot (v5.0). The experimental work can be viewed on the following link https://youtu.be/04844gWZA1E. The results obtained are satisfactory and motivating for the use of a torque to position transformer to implement robust controller.

Compliance with ethical standards

Conflicts of interest The authors declare that they have no conflict of interest.

References

1. Aldebaran robotics: Nao documentation. http://doc.aldebaran.com/2-1/family/nao_dcm/actuator_sensor_names.html. (Accessed on 08 April 2019)
2. Boiko I, Fridman L (2005) Analysis of chattering in continuous sliding-mode controllers. IEEE Trans Autom Control 50(9):1442–1446. https://doi.org/10.1109/TAC.2005.854655
3. Fallaha CJ, Saad M, Kanaan HY, Al-Haddad K (2011) Sliding-mode robot control with exponential reaching law. IEEE Trans Industr Electron 58(2):600–610. https://doi.org/10.1109/TIE.2010.2045995
4. Gelin R (2019) NAO. Springer, Dordrecht, pp 147–168. https://doi.org/10.1007/978-94-007-6046-2_14
5. Gouaillier D, Collette C, Kilner C (2010) Omni-directional closed-loop walk for nao. In: 2010 10th IEEE-RAS international conference on humanoid robots, pp 448–454. https://doi.org/10.1109/ICHR.2010.5686291
6. Hashemi E, Khajepour A (2017) Kinematic and three-dimensional dynamic modeling of a biped robot. Proc Inst Mech Eng Part K J Multi-body Dyn 231(1):57–73. https://doi.org/10.1177/1464419316645243
7. Kali Y, Rodas J, Gregor R, Saad M, Benjelloun K (2018) Attitude tracking of a tri-rotor UAV based on robust sliding mode with time delay estimation. In: ICUAS, international conference on unmanned aircraft systems
8. Khatib O, Thaulad P, Yoshikawa, Taizo, Park J (2008) Torque-position transformer for task control of position controlled robots. In: 2008 IEEE international conference on robotics and automation, pp 1729–1734. https://doi.org/10.1109/ROBOT.2008.4543450
9. Moosavian SAA, Takhmar A, Alghooneh M (2007) Regulated sliding mode control of a biped robot. In: 2007 international conference on mechatronics and automation, pp 1547–1552. https://doi.org/10.1109/ICMA.2007.4303779
10. Orozco-Soto SM, Ibarra-Zannatha JM (2017) Motion control of humanoid robots using sliding mode observer-based active disturbance rejection control. In: 2017 IEEE 3rd colombian conference on automatic control (CCAC), pp 1–8. https://doi.org/10.1109/CCAC.2017.8276383
11. Sanchez-Magos M, Ballesteros-Escamilla M, Cruz-Ortiz D, Salgado I, Chairez I (2019) Terminal sliding mode control of a virtual humanoid robot. In: 2019 6th international conference on control, decision and information technologies (CoDIT), pp 726–731. https://doi.org/10.1109/CoDIT.2019.8820326
12. Swikir A, Utkin V (2016) Chattering analysis of conventional and super twisting sliding mode control algorithm. In: 2016 14th international workshop on variable structure systems (VSS), pp 98–102. https://doi.org/10.1109/VSS.2016.7506898
13. Utkin V (1992) Sliding mode in control and optimization. Springer, Berlin
14. Utkin V, Guldner J, Shi J (1999) Sliding mode control in electromechanical systems. Taylor-Francis, Oxford
15. Yoshikawa T, Khatib O (2009) Compliant humanoid robot control by the torque transformer. In: 2009 IEEE/RSJ international conference on intelligent robots and systems, pp 3011–3018. https://doi.org/10.1109/IROS.2009.5353907
16. Youcef-Toumi K, Ito O (1990) A time delay controller for systems with unknown dynamics. ASME J Dyn Syst Meas Control 112:133–141